

## Numerical investigation of thermal performance and phase change of wax paraffin layer surrounding water tank

Mohammed A. Al Rawaf, Ph.D (Lecturer) \*

Jalal M. Jalil, Ph.D (Asst.Prof.) \*\*

### Abstract

Finite volume method was used to investigate the thermal performance and phase change of wax paraffin layers surrounding heated water tank (1 m cube). Different timing of heater power on (on and off hours) and different thickness (0.06, 0.1, 0.133 and 0.166 m) had been investigated. The investigation shows the required wax thicknesses necessary to keep the temperature of the wax paraffin layers within required range during periods of power off. Thickness of 0.1 m of paraffin wax with scheme (14 hours heater ON and 10 hours heater OFF) shows best performance among the other combinations. In this combination, reasonable working heater time (economic) and the temperature was kept nearly 50 C° along the whole period.

**Keywords:** Thermal Storage, Finite Volume, Wax Paraffin, Phases Change.

---

\* Al-Mansour University College

\*\* University of Technology

**Nomenclature:**

PCM=Phase Change Material

A =Area ( $m^2$ ).

a, b = coefficient in the discretization equation.

B='bottom' neighbor of grid P.

b=Control-volume face between P and B.

 $C_p$  = specific heat (kJ/kg °C). $C_{pl}$  =specific heat of liquid phase (kJ/kg °C). $C_{ps}$  =specific heat of solid phase (kJ/kg °C).

H =Enthalpy (kJ/kg).

e= Control-volume face between P and E.

E='east' neighbor of grid P.

L=latent heat (kJ/kg).

i, j, k=Unit vector.

k =thermal conductivity (W/ m °C).

 $k_l$  =liquid thermal conductivity (W/m °C). $k_s$  =solid thermal conductivity (W/m °C).

l=Liquid.

N='north' neighbor of grid P.

n=Control-volume face between P and N.

P=Grid point.

q=Heat generation ( $W/m^3$ ). $\bar{q}$  = Average heat generation.

S='south' neighbor of grid P.

s=Control-volume face between P and S.

s=Solid.

T =Temperature (°C).

t =Time(s).

 $T^*$  =Kirchhoff temperature (°C). $T_t$ ='Top' neighbor of grid P.

t = Control-volume face between P and T.

$T_m$  = melting temperature ( $^{\circ}\text{C}$ ).

$V$  = Volume ( $\text{m}^3$ ).

$W$  = west' neighbor of grid  $P$ .

$w$  = Control-volume face between  $P$  and  $W$ .

---

$x, y, z$  = Cartesian coordinates(  $\text{m}$ ).

$\rho$  =Density ( $\text{kg}/\text{m}^3$ ).

$\Delta x, \Delta y, \Delta z = x, y, z$  - Direction width of the control volume.

$\delta x, \delta y, \delta z = x, y, z$  -direction distance between two adjacent grid points.

$\lambda$  = Diffusion coefficient.

$\Delta$  =Difference.

$\partial$  =Partial derivative.

---

$\Delta T$  =Temperature range ( $^{\circ}\text{C}$ ).

## 1- Introduction

PCMs latent heat storage can be achieved through liquid–solid, solid–liquid, solid–gas and liquid–gas phase change. However, the only phase change used for PCMs is the solid–liquid change. Initially, the solid–liquid PCMs behave like **sensible heat** storage (SHS) materials; their temperature rises as they absorb heat. Unlike conventional SHS, however, when PCMs reach the temperature at which they change phase (their melting temperature) they absorb large amounts of heat at an almost constant temperature. The PCM continues to absorb heat without a significant rise in temperature until all the material is transformed to the liquid phase. When the ambient temperature around a liquid material falls, the PCM solidifies, releasing its stored latent heat. A large number of PCMs are available in any required temperature range from  $-5$  up to  $190^{\circ}\text{C}$ . A paraffin-wax used by Khin *et al.* has a melting point of  $62^{\circ}\text{C}$  and an enthalpy of fusion of  $145\text{--}240\text{ kJ/kg}$ . [1] Because water has a boiling point of  $100^{\circ}\text{C}$ , it will not undergo any change at  $62^{\circ}\text{C}$ . Therefore, water will be used as a low temperature non-PCM counterexample.

Hong *et al.* [2] tried to improve the accuracy of the T-history method for measuring heat of fusion of various materials and many of the PCMs were taken under study. Duffy [3] proposed a numerical simulation of porous latent heat thermal energy storage device for thermoelectric cooling under different porosities of the aluminum matrix. They used a porous aluminum matrix as a

way of improving the performance of the system, enhancing heat conduction without reducing significantly the stored energy. Ravikumar et al. [4] has proposed Cool storage system using phase change materials can be used for peak load shifting. Regin et al. [5] proposed a paper in analyzing the behavior of a packed bed latent heat thermal energy storage system

Trigui et al. [6] investigates Phase Change Material (PCM) composites based on low-density polyethylene (LDPE) with paraffin waxes were investigated in this study. The composites were prepared using a melt mixing method with a Brabender-Plastograph. Results indicate the performance of the proposed system is affected by the thermal effectiveness of phase change material and significant amount of energy saving can be achieved.

Thirugnanam and Marimuthu [7] investigated a double pipe type heat exchanger designed and fabricated for low temperature industrial waste heat recovery using Phase Change Material (PCM) paraffin wax (PW). The experimental results show the feasibility of using PCM as storage media in heat recovery systems. Regin et al. [8] analyzed the behavior of a packed bed latent heat thermal energy storage system. The packed bed is composed of spherical capsules filled with paraffin wax as PCM usable with a solar water heating system temperature range on the thermal performance of the capsules of various radii have been investigated. The results indicate that for the proper modeling of performance of the system the phase change.

Temperature range of the PCM must be accurately known, and should be taken into account. Nayak et al. [9] investigated the amount of convection and temperature change brought about due to the heat flux has been simulated and studied in detail by using GAMBIT and FLUENT .

In this numerical investigation, a Finite volume will used to calculate the necessary thickness of wax paraffin to keep the wax paraffin layers within acceptable range of temperature with four assumed schemes of heater working hours.

## 2. Numerical Formulations

Heat conduction problems with phase change were represented by Stefan problems. This problem is mathematically treated by the enthalpy transforming method; this method was proposed to convert the energy equation into a non-linear equation with a single dependent variable enthalpy (H). The advantage of the enthalpy method is that the problem is formulated in a fixed region to be solved. In addition to temperature; this method treats the enthalpy as a dependent variable and discretizes the energy equation into a set of equations that contain both temperature and enthalpy.

The analysis assumptions are:

1. Neglecting viscous dissipation,
2. Neglecting convection term, and
3. For each phase the specific heats are constant, where the phase change occurs at a single temperature. The analysis of the model in three-dimensions is related to Cao [10].

The energy equation is:

$$\frac{\partial}{\partial x} \left( k \frac{\partial T}{\partial x} \right) + \frac{\partial}{\partial y} \left( k \frac{\partial T}{\partial y} \right) + \frac{\partial}{\partial z} \left( k \frac{\partial T}{\partial z} \right) + \bar{q} = \rho \frac{\partial H}{\partial t} \quad \dots\dots\dots(1)$$

And the state equation,

$$\frac{dH}{dT} = C_p \quad \dots\dots\dots (2)$$

At constant specific heat case for each phase, and the phase change occurs at a single temperature [11],

$$T = \begin{cases} T_m + H / C_{ps} & H \leq 0 & \text{(Solid phase)} \\ T_m & 0 < H < L & \text{(Phase change)} \\ T_m + (H - L) / C_{pl} & H \geq L & \text{(Liquid phase)} \end{cases} \quad \dots\dots\dots(3)$$

For the above relation,  $H = 0$  was selected corresponding to phase change material (PCM) in their solid state to temperature  $T_m$ .

The "Kirchhoff" temperature is introduced as [12]:

$$T^* = \int_{T_m}^T k(\eta) d\eta = \begin{cases} k_s(T - T_m), & T < T_m \\ 0, & T = T_m \\ k_l(T - T_m), & T > T_m \end{cases} \quad \dots\dots\dots (4)$$

Transforming Equation (3), with the definition given in equation (4) results in next equation:

$$T^* = \begin{cases} k_s H / C_{ps}, & H \leq 0 \\ 0, & 0 < H < L \\ k_l (H - L) / C_{pl}, & H \geq L \end{cases} \quad \dots\dots\dots (5)$$

Now, introducing an enthalpy function as:

$$T^* = \lambda(H)H + S(H) \quad (6)$$

For the phase change in a single temperature,

$$\lambda(H) = \begin{cases} k_s / C_{ps}, & H \leq 0 \\ 0, & 0 < H < L \\ k_l / C_{pl}, & H \geq L \end{cases} \quad \dots\dots\dots(7)$$

And,

$$S(H) = \begin{cases} 0, & H \leq 0 \\ 0, & 0 < H < L \\ -Lk_l / C_{pl}, & H \geq L \end{cases} \quad \dots\dots\dots(8)$$

In terms of Kirchhoff temperature, Transforming equation (1) and substituting using equation (6), gives:

$$\rho \frac{\partial H}{\partial t} = \frac{\partial}{\partial x} \left( \frac{\partial(\lambda H)}{\partial x} \right) + \frac{\partial}{\partial y} \left( \frac{\partial(\lambda H)}{\partial y} \right) + \frac{\partial}{\partial z} \left( \frac{\partial(\lambda H)}{\partial z} \right) + p + q \quad \dots\dots\dots(9)$$

With

$$p = \frac{\partial}{\partial x} \left( \frac{\partial S}{\partial x} \right) + \frac{\partial}{\partial y} \left( \frac{\partial S}{\partial y} \right) + \frac{\partial}{\partial z} \left( \frac{\partial S}{\partial z} \right) \quad \dots\dots\dots(10)$$

For the liquid region away from the moving front, Equation (9) reduced to the normal linear energy equation:

$$\rho \frac{\partial H}{\partial t} = \frac{\partial}{\partial x} \left( k_l \frac{\partial T}{\partial x} \right) + \frac{\partial}{\partial y} \left( k_l \frac{\partial T}{\partial y} \right) + \frac{\partial}{\partial z} \left( k_l \frac{\partial T}{\partial z} \right) + q \quad \dots\dots\dots(11)$$

And in the solid region, Equation (9) reduces to:

$$\rho \frac{\partial H}{\partial t} = \frac{\partial}{\partial x} \left( k_s \frac{\partial T}{\partial x} \right) + \frac{\partial}{\partial y} \left( k_s \frac{\partial T}{\partial y} \right) + \frac{\partial}{\partial z} \left( k_s \frac{\partial T}{\partial z} \right) + q \quad \dots\dots\dots(12)$$

Without convection term in the phase change region, equation (9) reduces to:

$$\rho \frac{\partial H}{\partial t} = \frac{\partial^2}{\partial x^2} (\lambda H) + \frac{\partial S^2}{\partial x^2} + \frac{\partial^2}{\partial y^2} (\lambda H) + \frac{\partial S^2}{\partial y^2} + \frac{\partial^2}{\partial z^2} (\lambda H) + \frac{\partial S^2}{\partial z^2} \quad \dots\dots\dots(13)$$

For  $\lambda = \lambda(H)$  and  $S = S(H)$ , the above equation employs the control-volume finite-difference. In this methodology the discretization equation is obtained by using conservation laws over finite size control volume surrounding the grid nodes. Integrating the equation over the control volumes as:

$$\begin{aligned} \iiint_{\Delta V} \rho \frac{\partial H}{\partial t} \Delta V &= \iiint_{\Delta V} \frac{\partial}{\partial x} \left( \frac{\partial(\lambda(H))}{\partial x} \right) \Delta V + \iiint_{\Delta V} \frac{\partial}{\partial y} \left( \frac{\partial(\lambda(H))}{\partial y} \right) \Delta V + \iiint_{\Delta V} \frac{\partial}{\partial z} \left( \frac{\partial(\lambda(H))}{\partial z} \right) \Delta V \\ &+ \iiint_{\Delta V} \frac{\partial}{\partial x} \left( \frac{\partial S}{\partial x} \right) \Delta V + \iiint_{\Delta V} \frac{\partial}{\partial y} \left( \frac{\partial S}{\partial y} \right) \Delta V + \iiint_{\Delta V} \frac{\partial}{\partial z} \left( \frac{\partial S}{\partial z} \right) \Delta V + \iiint_{\Delta V} q \Delta V \quad \dots\dots\dots(14) \end{aligned}$$

Using an explicit scheme, the time variation term becomes,

$$\iiint_{\Delta V} \rho \frac{\partial H}{\partial t} \Delta V = \rho \Delta V \left( \frac{H_p - H_p^o}{\Delta t} \right) \quad \dots\dots\dots(15)$$

For x-direction from right hand side of equation (14) becomes

$$\iiint_{\Delta V} \frac{\partial}{\partial x} \left( \frac{\partial \lambda(H)}{\partial x} \right) \Delta V = \left[ \left( \frac{\partial \lambda(H)}{\partial x} \right)_e - \left( \frac{\partial \lambda(H)}{\partial x} \right)_w \right] \Delta y \Delta z = \frac{\Delta y \Delta z}{(\delta x)_e} (\lambda_E H_E - \lambda_p H_p) - \frac{\Delta y \Delta z}{(\delta x)_w} (\lambda_p H_p - \lambda_w H_w) \quad (16)$$

$$\iiint_{\Delta V} \frac{\partial}{\partial x} \left( \frac{\partial S}{\partial x} \right) \Delta V = \left[ \left( \frac{\partial S}{\partial x} \right)_e - \left( \frac{\partial S}{\partial x} \right)_w \right] \Delta y \Delta z = \frac{\Delta y \Delta z}{(\delta x)_e} (S_E - S_p) - \frac{\Delta y \Delta z}{(\delta x)_w} (S_p - S_w) \quad (17)$$

For y-direction from right hand side of equation (14) becomes

$$\iiint_{\Delta V} \frac{\partial}{\partial y} \left( \frac{\partial \lambda(H)}{\partial y} \right) \Delta V = \left[ \left( \frac{\partial \lambda(H)}{\partial y} \right)_n - \left( \frac{\partial \lambda(H)}{\partial y} \right)_s \right] \Delta x \Delta z = \frac{\Delta x \Delta z}{(\delta y)_n} (\lambda_N H_N - \lambda_p H_p) - \frac{\Delta x \Delta z}{(\delta y)_s} (\lambda_p H_p - \lambda_S H_S) \quad (18)$$

$$\iiint_{\Delta V} \frac{\partial}{\partial y} \left( \frac{\partial S}{\partial y} \right) \Delta V = \left[ \left( \frac{\partial S}{\partial y} \right)_n - \left( \frac{\partial S}{\partial y} \right)_s \right] \Delta x \Delta z = \frac{\Delta x \Delta z}{(\delta y)_n} (S_N - S_p) - \frac{\Delta x \Delta z}{(\delta y)_s} (S_p - S_S) \quad (19)$$

And for z-direction from right hand side of Equation (14) becomes

$$\iiint_{\Delta V} \frac{\partial}{\partial z} \left( \frac{\partial \lambda(H)}{\partial z} \right) \Delta V = \left[ \left( \frac{\partial \lambda(H)}{\partial z} \right)_t - \left( \frac{\partial \lambda(H)}{\partial z} \right)_b \right] \Delta x \Delta y = \frac{\Delta x \Delta y}{(\delta z)_t} (\lambda_T H_T - \lambda_p H_p) - \frac{\Delta x \Delta y}{(\delta z)_b} (\lambda_p H_p - \lambda_B H_B) \quad (20)$$

$$\iiint_{\Delta V} \frac{\partial}{\partial z} \left( \frac{\partial S}{\partial z} \right) \Delta V = \left[ \left( \frac{\partial S}{\partial z} \right)_t - \left( \frac{\partial S}{\partial z} \right)_b \right] \Delta x \Delta y = \frac{\Delta x \Delta y}{(\delta z)_t} (S_T - S_p) - \frac{\Delta x \Delta y}{(\delta z)_b} (S_p - S_B) \quad (21)$$

The last term from right hand side of equation (14) becomes

$$\iiint_{\Delta V} q \Delta V = \bar{q} \Delta V, \quad (22)$$

Now, the coefficient of  $H_N, H_S, H_E, H_W, H_T$  and  $H_B$  as  $a_N, a_S, a_E, a_W, a_T$  and  $a_B$ , respectively. Writing equation (15) in the familiar standard form:

$$a_p H_p = a_N H_N + a_S H_S + a_E H_E + a_W H_W + a_T H_T + a_B H_B + b \quad (23)$$

With,  $H_p^o$  denoting the old value of  $H$  at grid point P, the values of coefficients are:

$$a_p = a_N + a_S + a_W + a_E + a_T + a_B$$

$$a_E = \frac{\Delta t}{\rho \Delta V} \frac{\lambda_E A_x}{\delta x_e}, a_W = \frac{\Delta t}{\rho \Delta V} \frac{\lambda_W A_x}{\delta x_w}, a_N = \frac{\Delta t}{\rho \Delta V} \frac{\lambda_N A_y}{\delta y_n}, a_S = \frac{\Delta t}{\rho \Delta V} \frac{\lambda_S A_y}{\delta y_s}, a_T = \frac{\Delta t}{\rho \Delta V} \frac{\lambda_T A_z}{\delta z_t}, a_B = \frac{\Delta t}{\rho \Delta V} \frac{\lambda_B A_z}{\delta z_b} \quad (24)$$

$$A_x = \Delta y \Delta z, A_y = \Delta x \Delta z, A_z = \Delta x \Delta y, \Delta V = \Delta x \Delta y \Delta z$$

And,

$$b = -[a_N + a_S + a_E + a_W + a_T + a_B - 1] H_p^o + b_N S_N + b_S S_S + b_E S_E + b_W S_W + b_T S_T + b_B S_B - b_p S_p + \frac{dt}{\rho} q \Delta V \quad (25)$$

Where,

$$b_p = b_E + b_w + b_s + b_N + b_T + b_B$$

$$b_E = \frac{\Delta t}{\rho \Delta V} \frac{A_x}{\delta x_e}, b_w = \frac{\Delta t}{\rho \Delta V} \frac{A_x}{\delta x_w}, b_N = \frac{\Delta t}{\rho \Delta V} \frac{A_y}{\delta y_n}, b_s = \frac{\Delta t}{\rho \Delta V} \frac{A_y}{\delta y_s} \quad (26)$$

The last procedure is similar for liquid and solid regions for equations 11 and 12. The mesh is 31\*11\*11 in x, y, z directions and time step 10 second. First few mesh in x direction (3, 4, 5 and 6) are wax and the remaining are water. The properties of the wax paraffin are given in Table 1.

**Boundary Conditions:** The temperature of the first layer in x- direction was changed according to Table 2. The temperature is 80 C<sup>0</sup> when the heater is on and 25 C<sup>0</sup> when the heater is off. Boundaries surfaces in y and z direction were taken insulated. The initial conditions for all mesh are 25 C<sup>0</sup>. no load is assumed in the tank.

### 3- Results and Discussions

**Fig. 1** shows the behavior of isothermal contours for thickness 0.0166 m with time. Only x direction was appeared in the Fig. 1 due to there is no change in temperature in other directions (y, z). The temperature is starts to increase with time reaching maximum at time equals 14 hour (heater is on along this time). Then the temperature is starts to decreases until time equals 24 (heater is off from 14 to 24) where the heater is turn on again. The cycle is repeated for the next 24 hours.

**Fig. 2** shows average temperature of the wax layers with time for different thickness and

Scheme 1 (6 hour on and 18 hour off). To get benefit from wax layers, the temperature should reached 60 C<sup>0</sup> (melting temperature for wax) to store latent heat. The solid line (without symbols) represents the history of heater (on, off) and it's changed between 80 C<sup>0</sup> (heater on) and 25 C<sup>0</sup> (heater off). Minimum thickness 0.06 m reaches melting temperature but because the thickness is small, the temperature decreases dramatically to reach initial temperature 25 C<sup>0</sup> after the heater is shut off. This behavior make this thickness not suitable. The other thicknesses does not reach melting temperature so no latent heat is stored.

**Fig. 3** shows average temperature of the wax layers with time for different thicknesses and scheme 2 (10 hour on and 14 hour off). Similar behavior of Fig. 1, the minimum thickness 0.06 m reached melting temperature but declined quickly. Other thicknesses does not reach melting temperature to store latent heat.

**Fig. 4** shows average temperature of the wax layers with time for different thicknesses and scheme 3 (14 hour on and 10 hour off). In this scheme, both thicknesses 0.06 and 0.1 m reached melting temperature but the declines of 0.1 m is less than 0.06 so it seems that 0.1 m thickness is preferable.



**Fig. 5** shows average temperature of the wax layers with time for different thickness and

scheme 4 (18 hour on and 6 hour off). Three thicknesses (0.06, 0.1 and 0.133 m) reached melting temperature, two of them (0.06 and 0.1 m) cover the whole range with 60 C<sup>0</sup>. thickness 0.06 even stores complete latent heat and starts to claim to highest temperature (80 C<sup>0</sup>). This behavior is due to excess heat from long time of heater working. This scheme is not recommended because it is not economic.

### 3. Conclusions

- 1- The suitable of wax paraffin as thermal storage for its low melting temperature 60 C<sup>0</sup>.
- 2- The combination of thickness of 0.1 m and scheme 3 (14 hours on and 10 hours off) is suitable to keep the temperature within acceptable limit 50 C<sup>0</sup> and for economic issue.

### 4. References

- [1] Lane GA. Solar heat storage—latent heat materials, vol. I. Boca Raton, FL: CRC Press, Inc.; 1983.
- [2] Hong, H., Kim, S.K., Kim, Y.S. Accuracy improvement of t-history method for measuring heat of fusion of various materials. International Journal of Refrigeration 27: (2004) 360–366.
- [3] Trelles, J.P., Duffy, J.P, Numerical simulation of porous latent heat thermal energy storage for thermoelectric cooling. Applied Thermal Engineering 23: (2003) 1647–1664.
- [4] M.Ravikumar, PSS. Srinivasan, Phase change material as a thermal energy storage material for cooling of building, Journal of Theoretical and Applied Information Technology (2005) 503-512.
- [5] A. Felix Regin, S.C. Solanki, J.S. Saini, An analysis of a packed bed latent heat thermal energy storage system using PCM capsules: Numerical investigation, Renewable Energy 34 (2009) 1765–1773.
- [6] Abdelwaheb Trigui, Mustapha Karkri and Igor Krupa “Thermal conductivity and latent hat thermal energy storage properties of LDPE/wax as a shape-stabilized composite phase change material” *Energy Conversion and Management*, Volume 77, 2014.
- [7] Thirugnanam. C, Marimuthu. P. “Experimental Analysis of Latent Heat Thermal Energy Storage using Paraffin Wax as Phase Change Material” International Journal of Engineering and Innovative Technology (IJEIT) Volume 3, Issue 2, 2013.

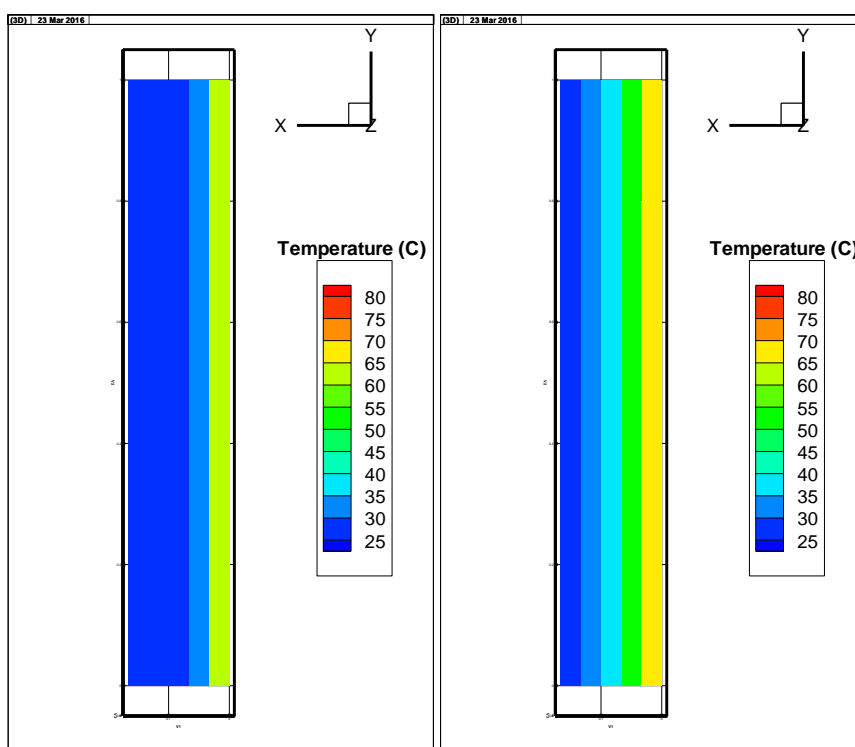
- [8] Felix Regin, S.C. Solanki, J.S. Saini "An analysis of a packed bed latent heat thermal energy storage system using PCM capsules: Numerical investigation" Renewable Energy 34 (2009) 1765–1773.
- [9] Amrit Om Nayak, M.Gowtham, R.Vinod, and G.Ramkumar "Analysis of PCM Material in Thermal Energy Storage System" International Journal of Environmental Science and Development, Vol. 2, No. 6, December 2011
- [10] Cao and Faghri., (1989), A numerical analysis of Stefan problems for generalized multi-dimensional phase change structure using the enthalpy transformation model, J. Heat Mass Transfer, Vol. 32, No. 7, PP. 1289-1298.
- [11] Norton T., Delgado A., Hogan E., Grace P., (2009), Simulation of high pressure freezing processes by enthalpy method, J. Food Engineering, Vol. 91, PP: 260-268.
- [12] S. Cho and J. Sunderland, "Heat-Conduction Problems with Melting or Freezing", J. Heat Transfer, PP. 421-425, 1962.

**Table 1** Physical properties of paraffin wax

Paraffin type	C22-C45
Melting temperature	56.8°C
Specific heat of solid	2.0 kJ/kg K
Specific heat of liquid	2.15 kJ/kg K
Latent heat of melting	190 kJ/kg
Thermal conductivity of solid	0.24 W/m.K
Thermal conductivity of liquid	0.22 W/m.K
Density of solid at 15°C	910 kg/m <sup>3</sup>
Density of liquid at 70°C	790 kg/m <sup>3</sup>

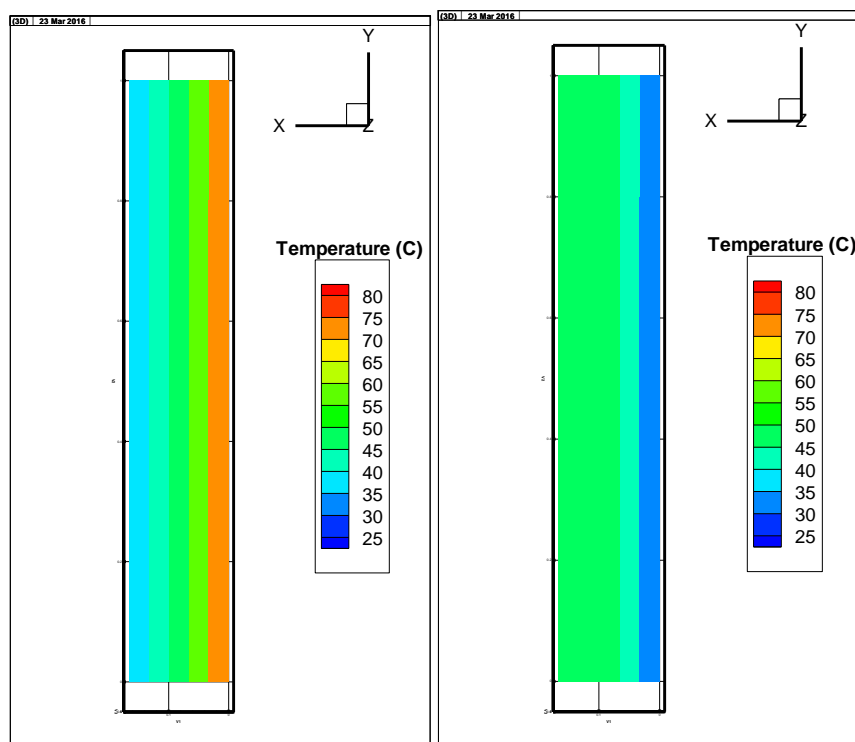
**Table 2** Time table of on- off heater working during 24 hours (first layer in x-direction)

Scheme	On (hr)	Off (hr)
1	6	18
2	10	14
3	14	10
4	18	6



Time = 1 hr

Time = 5 hr



Time = 10 hr

Time = 20 hr

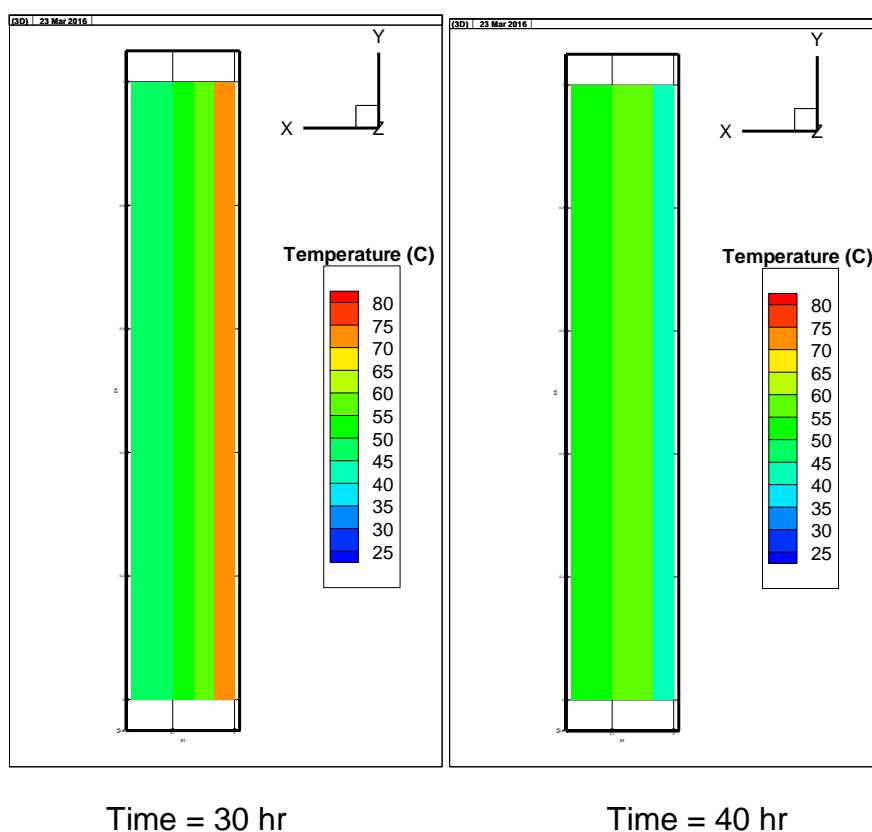


**Fig. 1** Isotherm contours at different time for thickness 0.166 m for boundary type 14.

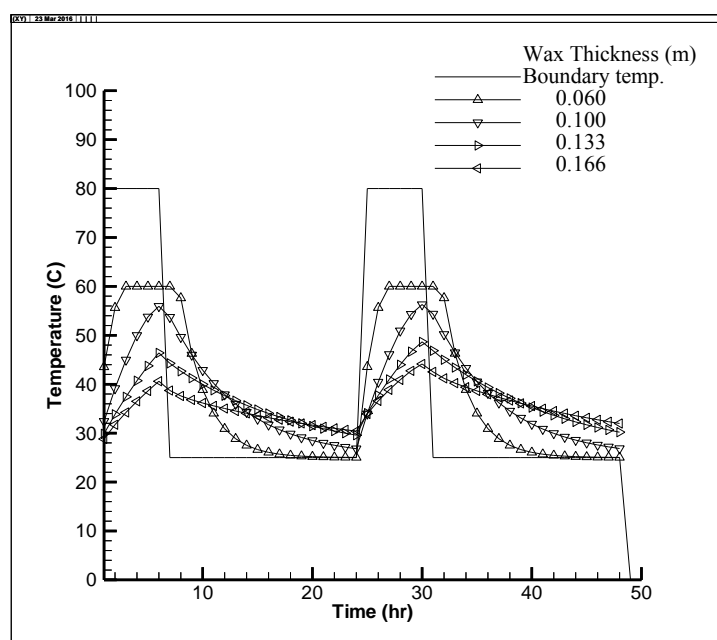


**Fig. 2** Average temperature variation of wax with different thickness, boundary type 1

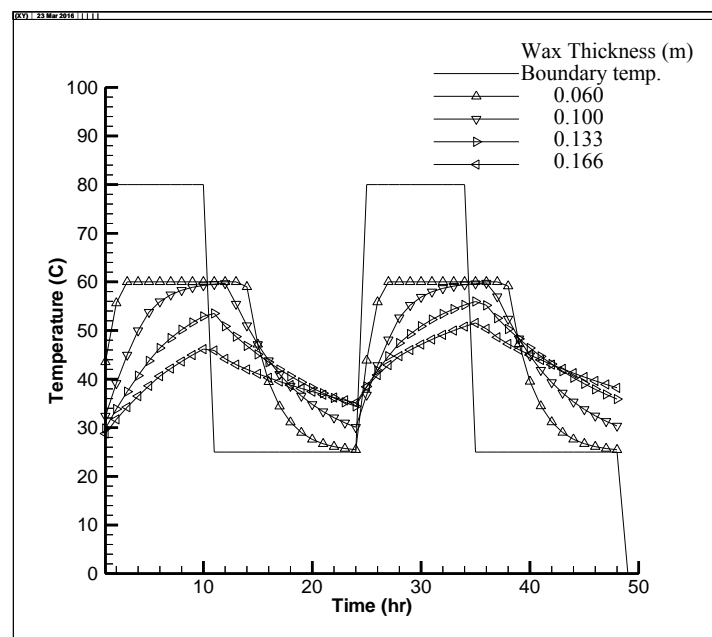


**Fig. 3** Average temperature variation of wax with different thickness, boundary type 2

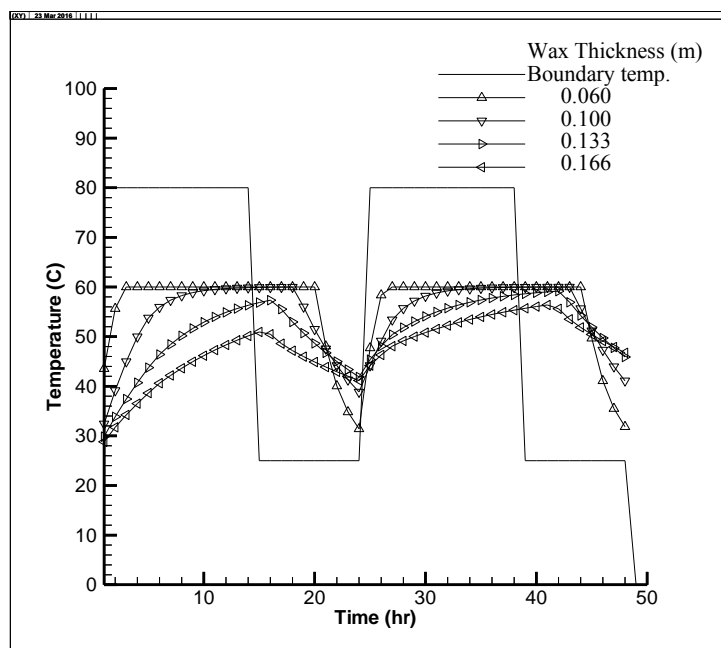


**Fig. 4** Average temperature variation of wax with different thickness, boundary type 3

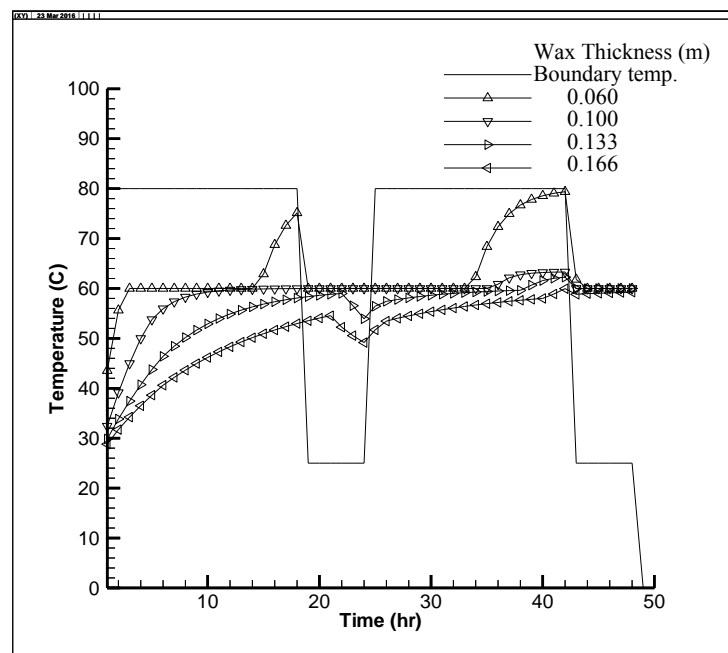


**Fig. 5** Average temperature variation of wax with different thickness, boundary type 4

## بحث رقمي لتغير الاداء الحراري وتغير طور طبقة شمع البرافين المحيطة بخزان ماء

م. د. محمد عبدالكريم الرواف \*

أ.د.جلال محمد جليل \*\*

### المستخلص

أستخدمت طريقة الحجم المحددة ( finite volume ) لدراسة الاداء الحراري وتغير الطور لمادة شمع البرافين المحيط بخزان ماء ساخن بحجم واحد متر مكعب حيث درست توقيتات متعددة لتشغيل واطفاء المسخن مع سماكات ( thicknesses ) مختلف لشمع البرافين (0.06, 0.1, 0.133, و 0.166 m) على التوالي. اظهرت النتائج ان سمك شمع البرافين للحفاظ على درجة الحرارة المطلوبة هو 0.1 m (خلال فترة تشغيل المسخن 14 ساعة وایقاف 10 ساعة) وهو الافضل بين السماكات الاخرى لتشغيل المسخن لفترة اقتصادية والحفاظ على درجة حرارة نحو 50 درجة مئوية خلال الفترة كلها.

\*كلية المنصور الجامعة

\*\*الجامعة التكنولوجية